Numerical study of propeller boss cap fins on propeller performance for Thai Long-Tail Boat

Prachakon Kaewkhiaw[*]

Department of Maritime Engineering, Faculty of International Maritime Studies, Kasetsart University, Sriracha Campus, 199 Moo 6, Sukhumvit Road, Tung Sukla, Si Racha, Chonburi 20230, Thailand

Abstract.　　The present paper purposes a numerical evaluation of the Thai Long-Tail Boat propeller (TLTBP) performance by without and with propeller boss cap fins (PBCF) in full-scale operating straight shaft condition in the first. Next, those are applied to inclined shaft conditions. The actual TLTBP has defined an inclined shaft propeller including the high rotational speed, therefore vortex from the propeller boss and boss cap (hub vortex) have been generated very much. The PBCF designs are considered to weaken of vortex behind the propeller boss which makes the saving energy for the propulsion systems. The blade sections of PBCF developed from the original TLTBP blade shape. The integrative for the TLTBP and the PBCF is analyzed to increase the performance using computational fluid dynamics (CFD). The computational results of propeller performance are thoroughly compared between without and with PBCF. Moreover, the effects of each PBCF component are computed to influence the TLTBP performance. The fluid flows around the propeller blades, propeller boss, boss cap, and vortex have been investigated in terms of pressure distribution and wake-fields to verify the increasing efficiency of propulsion systems.

Keywords:　computational fluid dynamics (CFD); inclined shaft propeller; propeller boss cap fins (PBCF); Thai Long-Tail Boat propeller (TLTBP); the Reynolds-averaged Navier-Stokes (RANS)

1. Introduction

The propeller boss cap fins (PBCF) are a type of energy-saving device for marine vessels which can diminish the vortex behind the boss cap therefore the efficiency of propulsion systems is improved. Long-Tail Boat can be many found in Southeast Asia Country, especially in Thailand, which is a boat native of the local people. The hull of the boat design to double steps for reducing the wetted surface area and the draft is low. It set the engine in the stern of the hull with an inboard where is connected to the long shaft. The long shaft is defined into the metal rod and the end of the shaft is the propeller. Thai Long-Tail Boat propeller (TLTBP) has a long time history to develop by local wisdom. It is divide into two blades with high pitch distribution.

The small vessels have must utilize an inclined shaft propeller including the Long-Tail Boat. TLTBP is a specific propeller and operating inclined shaft condition. The inclined shaft propeller and propeller boss cap fins have been interested in the experiment and the computational analysis by many researchers for a long time. The brief overviews of that are separated into the inclined shaft

---

*Corresponding author, Assistant Professor, E-mail: prachakon.ka@ku.th

condition and the PBCF condition. The measurement of inclined shaft propeller conditions such as Shields (1965) investigated the performance in open water tests with a series of five propellers operating the different inclined shaft angles, the five propellers are made the same designs but the different pitch ratios. Taniguchi *et al.* (1969) measured the propeller cavitation in oblique flow. Peck and Moore (1973) offered the horizontal and vertical side forces including the cavitation effect with inclined shaft propeller. Alder and Moore (1977) studied the comparison of the measured data of highly skewed propeller performance with inclined shaft partially-submerged propeller operating the different shaft yaw angles. The self-propulsion of planing craft with the outboard engine was purposed the hydrodynamic forces test operating inclined shaft angles by Katayama *et al.* (2013). Simultaneously, the marine propeller researchers investigated the phenomenal of flows around the inclined shaft propeller including the evaluation of the hydrodynamic performance by using numerical methods such as the unsteady propeller blade forces in different directions were predicted using the RANS by Krasilnikov *et al.* (2009). Schroeder and Dai (2010) described the CFD and experiment of unsteady analysis for propeller 4990 with operating the different inclined shaft angles, that results showed the propeller efficiency for an inclined shaft propeller are more than the straight shaft propeller. Dubbioso *et al.* (2013) presented the numerical method to analyze propeller performance in oblique flow by using the INSEAN E779A propeller model. Besides, the LTBP performance operating straight and inclined shaft conditions in model cases has been examined by Kaewkhiaw *et al.* (2015, 2016). After that, the unsteady propeller performance operating the different inclined shaft angles is analyzed by Kaewkhiaw (2020). Also, Gaggero and Villa (2018) predicted the non-cavitating and cavitating unsteady performances of the Potsdam Propeller Test Case (PPTC) in oblique flow with the OpenFOAM RANS calculations. Next, the investigation for the effect of inclined shaft angles on noise of cavitating on DTMB 4119 propeller is studied by Bal (2020).

Meanwhile, the computation and experiment in propeller boss cap fins (PBCF) are interested by many researchers in the long history. A brief summary of that mention such as Nojiri *et al.* (2011) described the effect of the PBCF in open water test (POT) and CFD analysis, the results can be reduced the fuel consumption in full-scale ships. The numerical analysis of hub effect on the hydrodynamic performance of propellers with the inclusion of PBCF to equalize the induced velocity is presented by Ghassemi *et al.* (2012). Kawamura *et al.* (2012) offered the CFD analysis of PBCF for two different propellers with model and full-scale propellers. Peng *et al.* (2013) studied integrative between propeller and PBCF in theory and numerical optimization design. Lim *et al.* (2014) performed to analyze the propulsion efficiency with the different boss cap fins model for container ships. The optimization of energy-saving devices (Turbo-Ring) with a propeller using a real-coded genetic algorithm compared to the experiment is conducted by Ryu *et al.* (2014). The PBCF design parameter for propeller efficiency and characteristics of the wake-field with propeller boss cap fins in hub vortex reduction is purposed by Seo *et al.* (2016). Also, Sun *et al.* (2016) determined the impact of PBCF on the hydrodynamic performance and flow field distribution of the propeller with a rudder. Next, numerical analysis of the inclined angle of propeller boss cap fins with two types of hubs on propeller performances is offered by Abar and Utama (2019).

The PBCF has never been studied to apply with TLTBP including to study with the effective by theory therefore this paper presents the numerical analysis of the TLTBP performance operating without and with PBCF in full-scale size of the Reynolds number operating straight shaft condition. After that, those are applied to an inclined shaft angle by using the RANS. Besides, each component of PBCF has been evaluated to effects the propeller performance. The integrative for the TLTBP and PBCF has been considered by increasing the efficiency of the propulsion system. The PBCF shapes
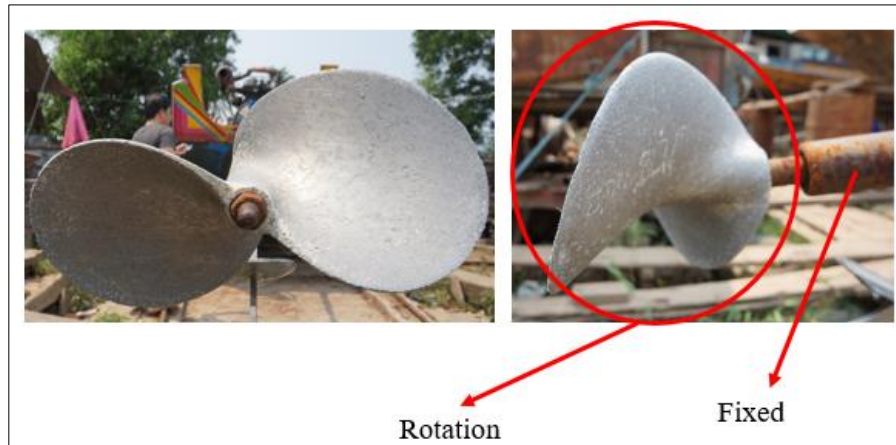
Fig. 1 The photograph of TLTBP at front view (left) and side view (right)

are generated from the original TLTBP blade. The computational results of the propeller performance without and with PBCF are compared to each other including an investigation of the pressure distribution and wake-field behind PBCF regions. Finally, those results will be applied to modify with a Thai Long-Tail Boat in the future.

2. Thai Long-Tail Boat propeller (TLTBP) and propeller boss cap fins (PBCP)

The actual TLTBP operating inclined shaft angle by approximately $12°$ to the horizontal axis is employed to the boat as shown in Fig. 1. The TLTBP principal particulars and geometry parameters are presented in Table 1. The numerical studies in this work are carried out in full-scale propeller, Fig. 2 shows the propeller and other components in the computation which has been generated as same as the original TLTBP. However, the hydrodynamic propeller performance in the open water test of the TLTBP model scale was measured for operating straight shaft conditions in the high-speed circulating water channel at Kyushu University by Kaewkhiaw *et al.* (2015).

Fig. 3 shows the flows phenomenal and force components operating inclined shaft propeller with TPBCF corresponding to this research. The inflow velocity, V_a divide into two components of the propeller plane, the first is $V_a cos\varphi$ in the shaft axial and flow speed will be reduced more than to normal inflow. The second, $V_a sin\varphi$ in vertical of the propeller shaft which is influenced to inducing the central of propeller thrust eccentricity. Where φ is the inclined shaft angles to the horizontal axis. On the one side, the propeller will generate the axial thrust, T which can be separated into two components. First, $Tcos\varphi$ is a force to push the boat in a horizontal axial. The second, $Tsin\varphi$ is vertical and it makes to the unbalance force and momentum then may motive the trim for inclined shaft condition. The PBCF will generate the axial thrust, t which is adverse to the axial thrust of a propeller, T therefore it is drag force. The axial thrust of the PBCF can be divided into two components. First, t$cos\varphi$ at horizontal axial which is the opposite direction to $Tcos\varphi$. Second, t$sin\varphi$ at vertical and it is the opposite direction to $Tsin\varphi$, thereby is an advantage to reduce the trim angle at the stern. Besides, the PBCF generates contrary torque to propeller torque, therefore it diminishes the total torque.
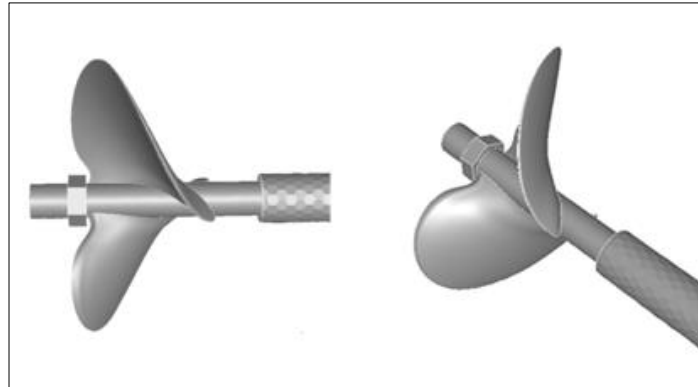
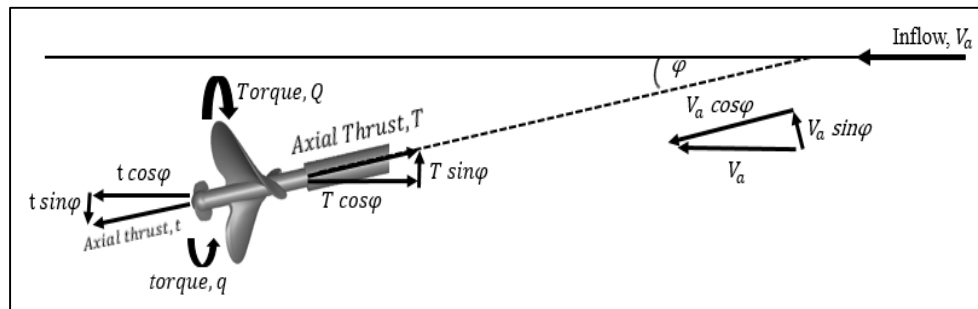Fig. 2 Full-scale TLTBP at side view (left) and Isometric view (right)

Fig. 3 Flow velocity and force generation diagram for TLTBP with PBCF

The principal particulars of propeller boss cap fins (PBCF) were developed from the TLTBP by keeping the blade section ratio to as same the TLTBP in the radial directions but the pitch distributions, rake distributions, and skew angles are changed. The vortex from the propeller boss and boss cap (hub vortex) in downstream will collapse by the hypothesis of PBCF geometry design. The many fins have been calculated to adopt integrative with TLTBP for increasing the performance of propulsion. Finally, there present two models are satisfied and it is described in Table 2. Fig. 4 and 5 show the TLTBP geometry with PBCF-A and TLTBP with PBCF-B respectively.

3. Numerical modeling

The numerical methods in this work were followed the previous research by the authors. Fluid flows are simulated to rotate around TLTBP and PBCF by moving interface systems in steady states. The governing equations are based on the Reynolds-averaged Navier-Stokes equations (RANS). The k-ω SST (shear stress transport) turbulence model is adopted to the Reynolds-stress terms in the RANS equations. The computational fluid dynamics code Ansys Fluent was carried out to solve the problems. The pressure-velocity coupling is accomplished through the SIMPLE algorithm. The Second Order Upwind scheme is employed for the discretization of the momentum equation. Details of the numerical modeling have been applied in this work which can be found by Kaewkhiaw *et.al* (2015, 2016, 2020).

Table 1 Specifications of TLTBP in full-scale

Number of blades: 2

Diameter (mm): 340

Hub diameter ratio: 0.14

Expanded area ratio: 0.6

Shaft length (m): 4.5

Inclined shaft angle (°): 12

Direction of rotation: Right Hand

Design advance coefficient (J): 1.1

Reynolds number: 2.88E+06 - 6.40E+06

Propeller geometry parameters

r/R	P/D	Rake/D	Skew(°)	c/D
0.14	0.873	-0.013	0.000	0.458
0.20	0.909	0.010	0.000	0.501
0.30	1.018	0.021	6.768	0.541
0.40	1.101	0.027	11.570	0.600
0.50	1.192	0.035	15.679	0.621
0.60	1.221	0.042	19.593	0.613
0.70	1.260	0.048	22.585	0.583
0.80	1.268	0.051	24.925	0.519
0.90	1.274	0.055	27.328	0.392
0.95	1.278	0.059	28.930	0.273
0.99	1.244	0.061	29.571	0.114
1.00	1.206	0.062	29.571	0.044

Table 2 Parameters of PBCF

Fin Types	Diameter (mm)	Fin numbers	r/R	P/D	c/D
			0.3	1.2	0.62
A	90	2	0.6	1.2	0.58
			1.0	1.1	0.30
			0.3	1.2	0.50
B	102	2	0.6	1.2	0.58
			1.0	1.1	0.45

4. Computational domains and grids generation

The flow field of TLTBP with PBCF operating inclined shaft propeller is non-equilibrium due to the cross-flow component in the influx of the shaft direction. Moreover, influence forces between

the TLTBP and PBCF have interacted therefore the whole domains were applied to computational domains. The domains of calculation are split out into two components. First, the outer domain with the stationary region. Second, the inner domain with a rotational region that is responded to rotate for the TLTBP and PBCF. Fig. 6 shows the computational domains. The inflows velocity, V_a is
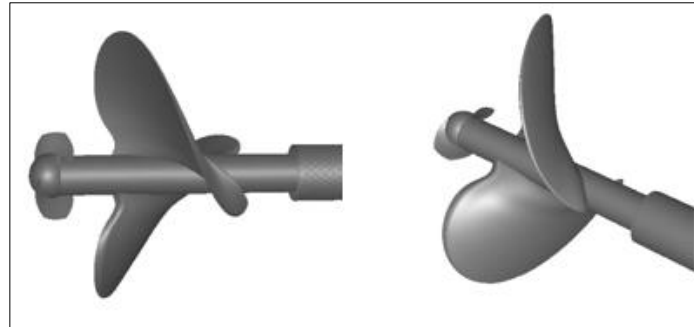

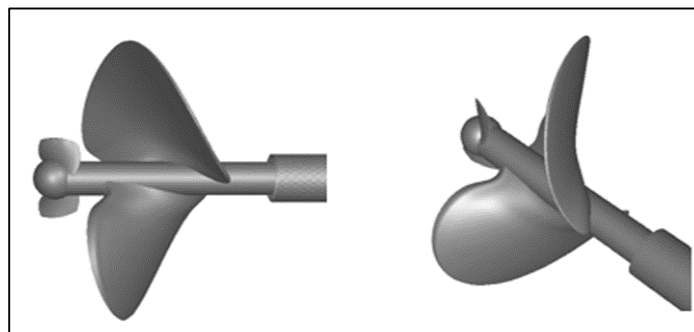Fig. 4 TLTBP with PCBF-A arrangement at side view (left) and Isometric view (right)

Fig. 5 TLTBP with PCBF-B arrangement at side view (left) and Isometric view (right)

Table 3 Dimension of computational domains for TLTBP with PBCF

	Stationary	Rotational
D1		1.50D
D2	8.80D	
L1		1.20D
L2	27.10D	

Table 4 Grids of computational domain for TLTBP with PBCF

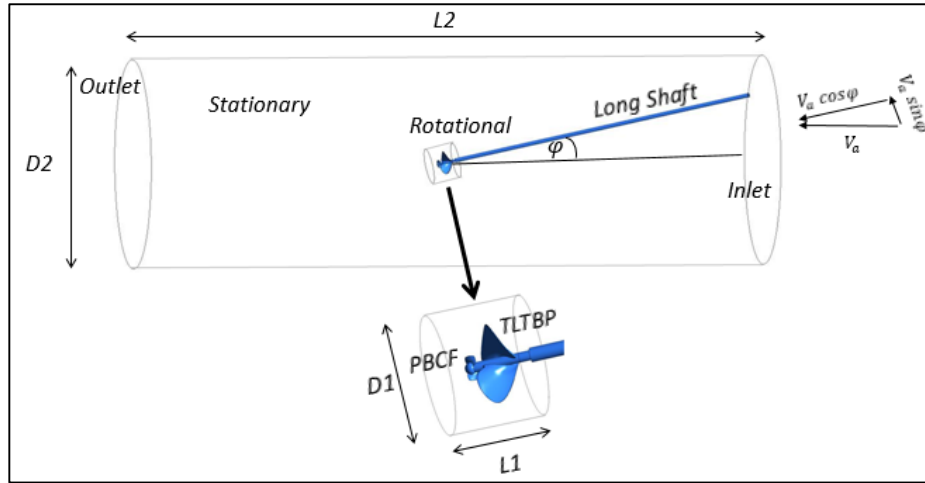| Names	Grid Types	LTBP+PBCF-A		LTBP+PBCF-B	
		Cells	Stationary	Rotational	Stationary
Preliminary	Coarse	1.2M	0.5M	1.2M	0.5M
Baseline	Medium	2.2M	1M	2.2M	1M
Refined	Fine	3.2M	2M	3.2M	2M

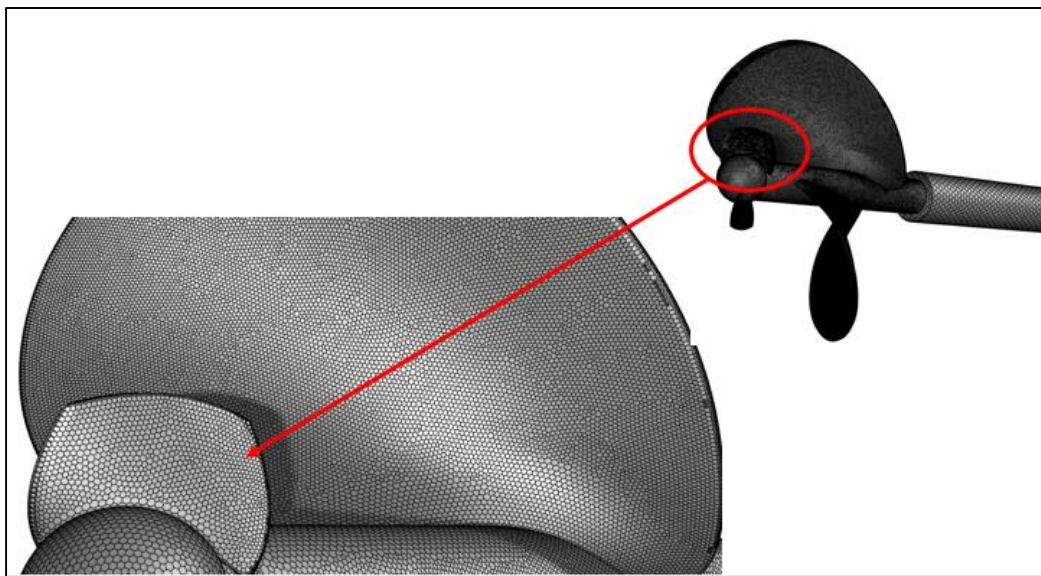Fig. 6 Computational domain of TLTBP with PBCF operating inclined shaft angle

Fig. 7 Computational polyhedral grids on TLTBP with PBCF

decomposed into shaft axial direction where is $V_a cos\varphi$, $V_a sin\varphi$ imposed into vertical. The outlet is set to pressure in the far-field. The mass and momentum equations are transferred by the moving interface domains. The dimension of computational domains is determined in Table 3 which has been studied by Kaewkhiaw (2020).

    The calculation domains for an inclined shaft of TLTBP with PBCF are divided into discrete control volumes by the polyhedral grids which have high flexibility to fit the complex geometry of the propeller and boss cap fins. The TLTBP and PBCF surfaces are conducted to finesse grids and to apply the boundary prism layers on near surfaces of them for solving the viscous layer. The surrounding surfaces areas created the larger grids. Fig. 7 shows the computational grids on the
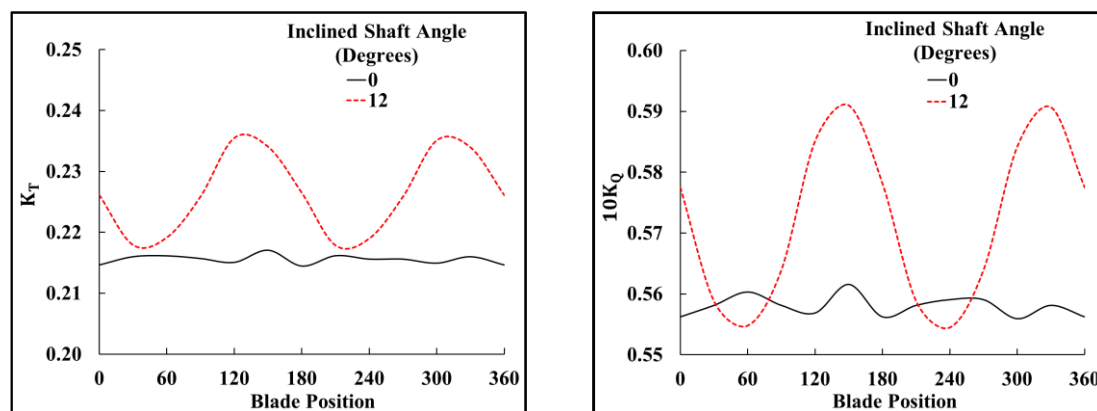
Fig. 8 Comparison of thrust (left) and torque coefficients (right) on all blades as functions of blade position at design advance coefficient with operating the straight shaft and inclined shaft conditions (Kaewkhiaw 2020)

TLTBP with PBCF. The grid quality presents in Table 4, grid independence is studied to precise for computational results by separation into three conditions, the first is called the preliminary grids which are coarse mesh. Second, it is applied to the baseline grids which are medium mesh. Finally, it is modified to finesse mesh, it is called the refined grids. The adaptive mesh refinement techniques have been applied to them. The first layer thickness of the prism layer is determined to a non-dimensional wall distance on surfaces of the TLTBP and PBCF. The other layers are defined to increase the rate of prism layer thickness. The average values of y^+ on the solid surfaces (TLTBP and PBCF) were kept below 30 for the refined grids (Kaewkhiaw *et al.* 2016).

5. Results and analysis

The numerical results of TLTBP operating straight shaft and inclined shaft conditions for the model scale of Reynolds number have been studied in previous research by Kaewkhiaw *et al.* (2016, 2020). That mention, the computational results of thrust and torque coefficients on all blades as one rotational with operating the different inclined shaft angles were compared to each other, which is demonstrated in Fig. 8, the more details of that results described by Kaewkhiaw (2020).

Computational results of the full-scale in this research were computed the propeller performance to compare with the model scale including the experimental data at each range of advance coefficients for check grids quality in the first, which presented in Fig. 9. The grid independence is evaluated for the accuracy results, where are called the Preliminary, the Baseline and the Refined. It found that the precision of calculations for the Refined grids is better than the Preliminary and Baseline grids. The thrust coefficients for full-scale with the Refined have agreed well to model-scale including experiment, the torque coefficients are slightly increased to model-scale, and the measurement at higher advance coefficients. However, the propeller efficiency of the full-scale and model-scale is a good agreement, especially at the design advance coefficient, J=1.1.

Henceforth, the computational results of the full-scale in this research only focused on the Refined grid where is separated into two conditions. First, the evaluation of the propeller performance of TLTBP in straight shaft condition between without PBCF and with PBCF comparing
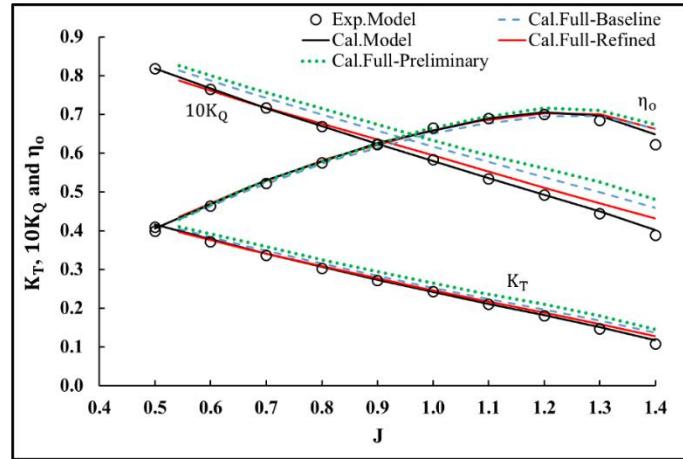
Fig. 9 Comparison of propeller performance between the full-scale and model-scale for TLTBP (without PBCF) operating straight shaft condition
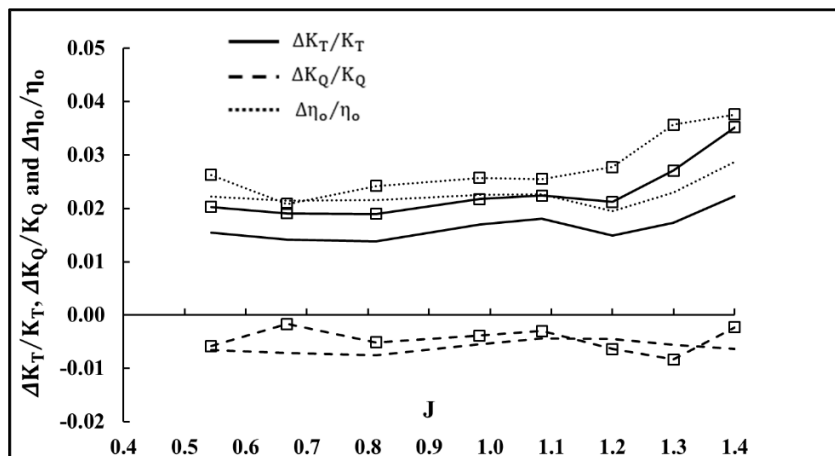

Fig. 10 Comparison between the effects of PBCF-A (line without symbol) and PBCF-B (line with symbol) for the TLTBP propeller performance in full-scale operating straight shaft condition

to each other. Next, it has been applied to investigate propeller performance an inclined shaft angle between without PBCF and with PBCF. The shaft length is defined into the same as actual TLTBP.

The integrative between TLTBP and PBCF models is studied to increasing propulsive efficiency with numerical results. However, the two PBCF models are satisfied to be suitable, which are the PBCF-A and PBCF-B.

5.1 The straight shaft condition

The phenomenal of acting forces considered to same as the flow and force diagram in Fig. 3 but the inclined shaft angle is zero, $\varphi = 0$. The effects of the PBCF for the TLTBP have been computed in terms of the relation to change for the thrust, torque coefficients, and the propeller efficiency where are defined by the following equation.
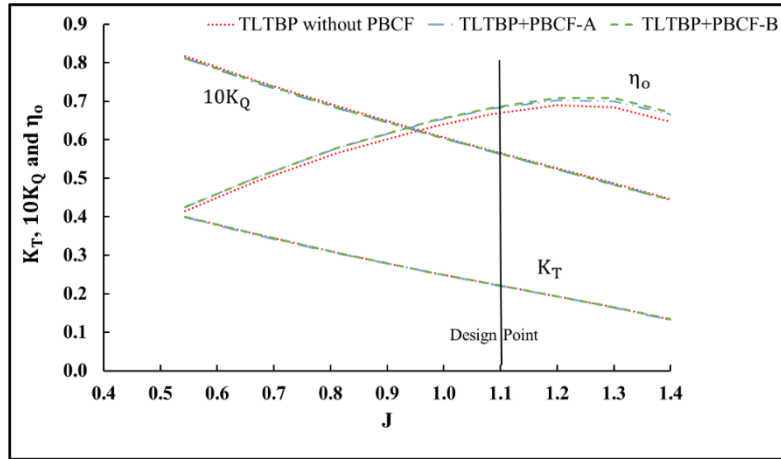
Fig. 11 Comparison of TLTBP propeller performance between without PBCF and with PBCF in full-scale operating straight shaft condition

$$\frac{\Delta K_T}{K_T} = \frac{K_T'-K_T}{K_T}, \frac{\Delta K_Q}{K_Q} = \frac{K_Q'-K_Q}{K_Q} \text{ and } \frac{\Delta \eta_o}{\eta_o} = \frac{\eta_o'-\eta_o}{\eta_o} \tag{1}$$

Where, K_T, K_Q and η_o are the thrust, torque coefficients, and propeller efficiency without PBCF respectively. The K_T', K_Q' , and η_o' are that by with PBCF.

The effects of the PBCF-A and PBCF-B on the TLTBP performance are presented in Fig. 10. It is seen that the thrust coefficients of the propeller with the PBCF-A and PBCF-B increased by about 1.4% - 2.2% and 2.0% - 3.5% respectively. The torque coefficients of both decreased to all. As a result, the propeller efficiency of PBCF-A showed to increase by about 1.9% - 2.9%. However, it seemed the propeller efficiency of PBCF-B is showed higher than PBCF-A and that values by approximately 2.1% - 3.8%. Also, the efficiency of PBCF-B is better than PBCF-A at the design advance coefficient, J=1.1. The reason for those results, it has likely seemed the fins shape of PBCF-B to be suitable with TLTBP more than the PBCF-A. Fig. 11 shows the thrust, torque coefficients, and propeller efficiency at each range of advance coefficients between without PBCF and with PBCF. That results have corresponded in Fig. 10. At the design point, the efficiency of PBCF-A and PBCF-B are increased by approximately 2.3% and 2.5% respectively.

Furthermore, the overall thrust and torque coefficients can be decomposed in the computational results which are expressed by the following equations.

$$K_T(\text{Total}) = K_T(\text{Propeller Blades}) + K_T(\text{Boss}) + K_T(\text{Boss Cap}) + K_T(\text{Long Shaft}) + K_T(\text{Fins}) \tag{2}$$

$$K_Q(\text{Total}) = K_Q(\text{Propeller Blades}) + K_Q(\text{Boss}) + K_Q(\text{Boss Cap}) + K_Q(\text{Long Shaft}) + K_Q(\text{Fins}) \tag{3}$$

Where, $K_T(\text{Propeller Blades})$, $K_T(\text{Boss})$, $K_T(\text{Boss Cap})$, $K_T(\text{Long Shaft})$, and $K_T(\text{Fins})$ are the contribution to the thrust coefficients of propeller blades, boss, boss cap, long shaft, and fins respectively. The torque coefficients of there can be decomposed to the same as thrust coefficients. The relative changing of the thrust coefficient due to the PBCF effects is determined by the following equation.
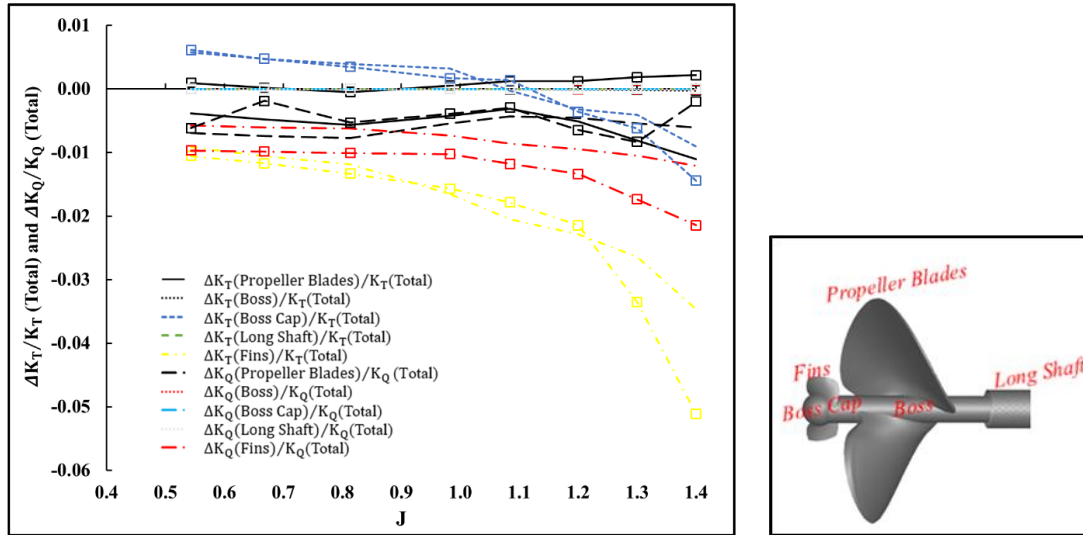
Fig. 12 Comparison of the effects in each component between PBCF-A (line without symbol) and PBCF-B (line with symbol) for the TLTBP operating straight shaft condition

$$\frac{\Delta K_T}{K_T(Total)} = \frac{\Delta K_T(Propeller\ Blades)}{K_T(Total)} + \frac{\Delta K_T(Boss)}{K_T(Total)} + \frac{\Delta K_T(Boss\ Cap)}{K_T(Total)} + \frac{\Delta K_T(Long\ Shaft)}{K_T(Total)} + \frac{\Delta K_T(Fins)}{K_T(Total)} \quad (4)$$

$$\frac{\Delta K_Q}{K_Q(Total)} = \frac{\Delta K_Q(Propeller\ Blades)}{K_Q(Total)} + \frac{\Delta K_Q(Boss)}{K_Q(Total)} + \frac{\Delta K_Q(Boss\ Cap)}{K_Q(Total)} + \frac{\Delta K_Q(Long\ Shaft)}{K_Q(Total)} + \frac{\Delta K_Q(Fins)}{K_Q(Total)} \quad (5)$$

Where, $\Delta K_T(Propeller\ Blades)$, $\Delta K_T(Boss)$, $\Delta K_T(Boss\ Cap)$, and $\Delta K_T(Long\ Shaft)$ are the changing of $K_T(Propeller\ Blades)$, $K_T(Boss)$, $K_T(Boss\ Cap)$, and $K_T(Long\ Shaft)$ by the effect of PBCF. While $\Delta K_T(Fins)$ is the thrust coefficient of the fins. The relative changing of the torque coefficients can be defined by the same as thrust coefficients.

Each component analysis of PBCF-A and PBCF-B for the TLTBP is shown in Fig. 12. It found the $\Delta K_T(Propeller\ Blades)$ for the PBCF-A are always negative and its values vary by about 0% - 1% of $K_T(Total)$ but the PBCF-B, $\Delta K_T(Propeller\ Blades)$ are mostly positive but its value is small. $\Delta K_T(Boss)$ and $\Delta K_T(Long\ Shaft)$ for both PBCF are similar tendencies and the values are small. The $\Delta K_T(Boss\ Cap)$ for both PBCF are almost similar, the magnitudes show positive at the range of lower advance coefficients but it shows negative at the range of higher advance coefficients. The $\Delta K_T(Fins)$ is always negative with both PBCF and its value vary by about 1% - 5% of $K_T(Total)$, the PBCF-B is changed to an extreme at higher advance coefficients. Therefore, the fins shape of the PBCF-B is seemed to match with the propeller more than PBCF-A.

It seemed $\Delta K_Q(Propeller\ Blades)$ with both PBCF are always negative and the values are not many different by approximately 0% - 1% of $K_Q(Total)$. The $\Delta K_Q(Boss)$, $\Delta K_Q(Boss\ Cap)$, and $\Delta K_Q(Long\ Shaft)$ with both PBCF are similar and the magnitudes are very low. The $\Delta K_Q(Fins)$ with both PBCF are showed negative at all by about 0.6% - 2.1% of the $K_Q(Total)$. However, it found the magnitudes of PBCF-B are higher than PBCF-A at each range of advance coefficients.

These results are found that $\Delta K_T(Propeller\ Blades)$ has slightly increased but $\Delta K_Q(Propeller\ Blades)$ has decreased, the magnitudes of $\Delta K_Q(Fins)$ can be subsided the
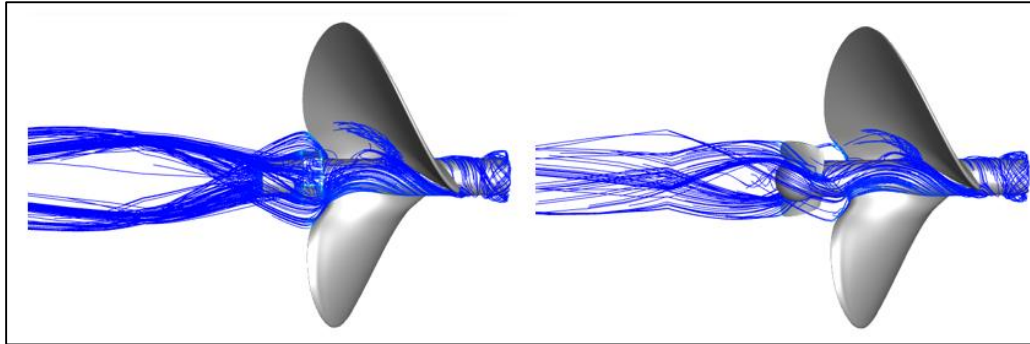
Fig. 13 Streamlines behind the boss cap of TLTBP without PBCF (left) and with PBCF-B (right) at design advance coefficient, J=1.1
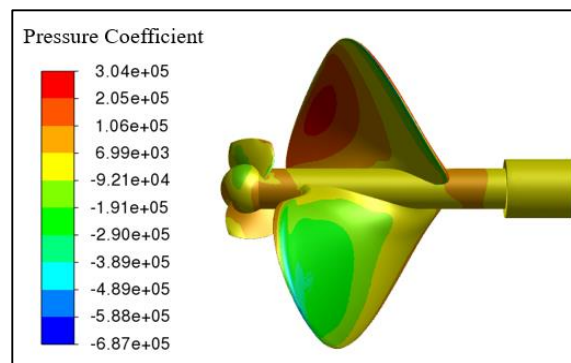

Fig. 14 Pressure distributions on the surface blades of TLTBP with PBCF-B at design advance coefficient, J=1.1

propeller torque while the values of the others are small therefore the propeller efficiency is increased.

The comparison of streamlines at behind areas of the boss cap between without PBCF and with PBCF-B operating at design advance coefficient is described in Fig. 13. It is seen in the case of without PBCF, vortex flows are rotated in as same propeller direction which seemed very vehement and long swirl around the end of the boss cap and after areas, the reason is grown up the hub vortex. However, in the case of PBCF-B, vortex flows around boss cap including after areas have been diminished, it observed to reduce aggressive of hub vortex in downstream of the boss cap.

Fig. 14 shows the pressure distributions on the TLTBP and PBCF-B. The pressure on the fins generated thrust and torque in the opposite direction to the propeller blades which corresponded in Fig. 13. Therefore, those results indicate that the flow characteristics have been subsided vortex behind the boss and boss cap.

5.2 The Inclined shaft condition

Inclined shaft propeller is an original condition for the Thai Long-Tail Boat, it defines about 12° from the horizontal axial. The phenomenal of acting forces have corresponded to the flow and force
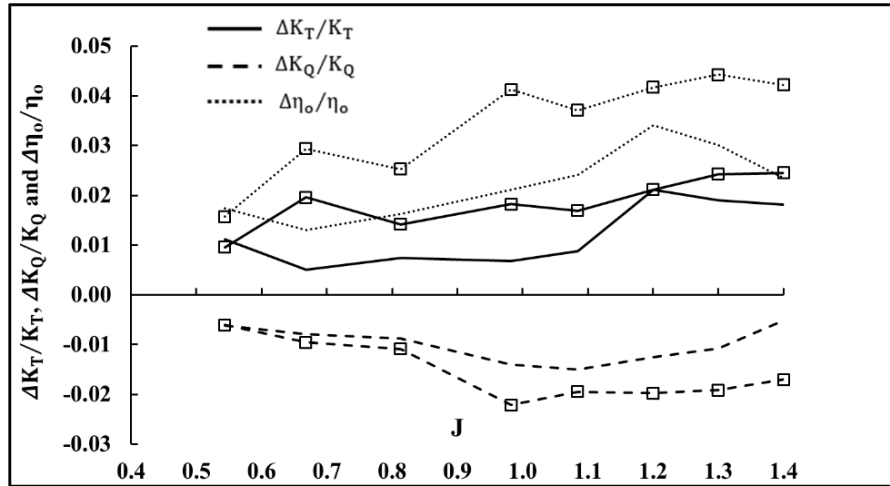
Fig. 15 Comparison between the effects of PBCF-A (line without symbol) and PBCF-B (line with symbol) for the TLTBP propeller performance in full-scale operating inclined shaft condition
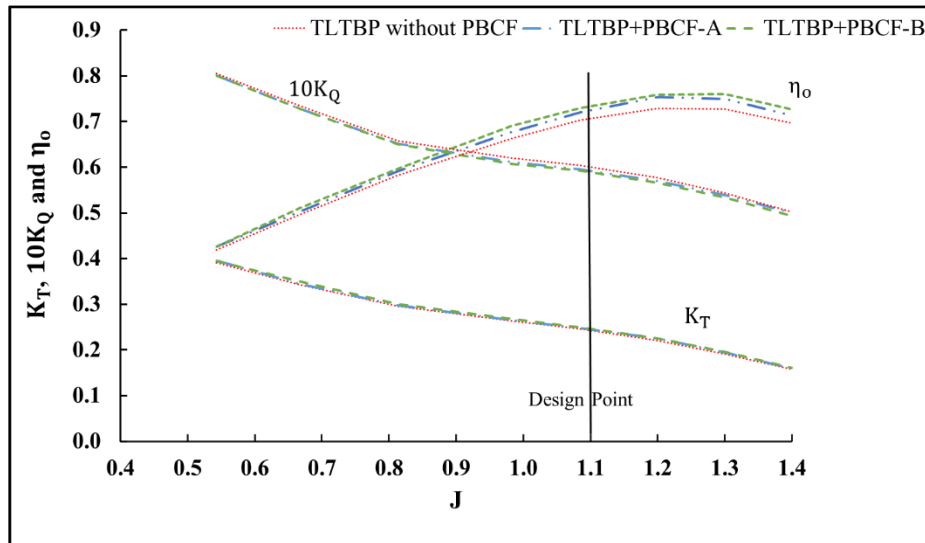

Fig. 16 Comparison of TLTBP propeller performance between without PBCF and with PBCF in full-scale operating inclined shaft condition

diagram in Fig. 3. The effects of each component with PBCF for the TLTBP have been calculated using as same as the equations of the straight shaft condition. The forces and moments are converted in an inflow direction which makes the running boat. The effects of the PBCF-A and PBCF-B on TLTBP performance are displayed in Fig. 15. It found the thrust coefficients of the propeller with the PBCF-A and PCBF-B were grown by approximately 0.5% - 2.1% and 1.0% - 2.6% respectively. Torque coefficients of the propeller with PBCF-A and PBCF-B seemed to decrease by about 0.6% - 1.5% and 0.6% - 2.2% respectively. Therefore, the efficiency of the propeller for PBCF-A and PBCF-B increased by about 1.3% - 3.4% and 1.6% - 4.4% respectively. However, it looks like that
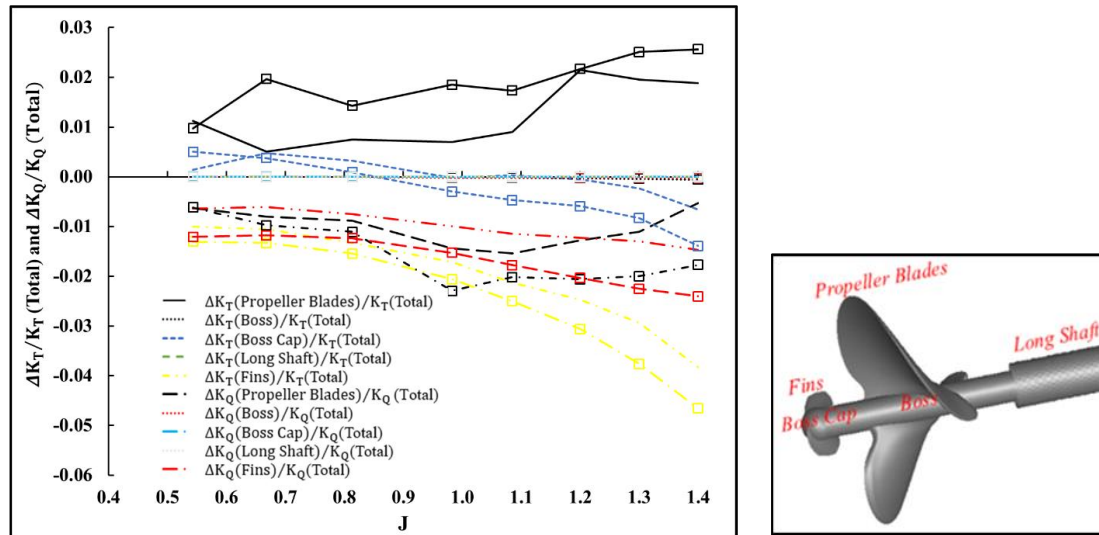
Fig. 17 Comparison of the effects in each component between PBCF-A (line without symbol) and PBCF-B (line with symbol) for the TLTBP operating inclined shaft condition
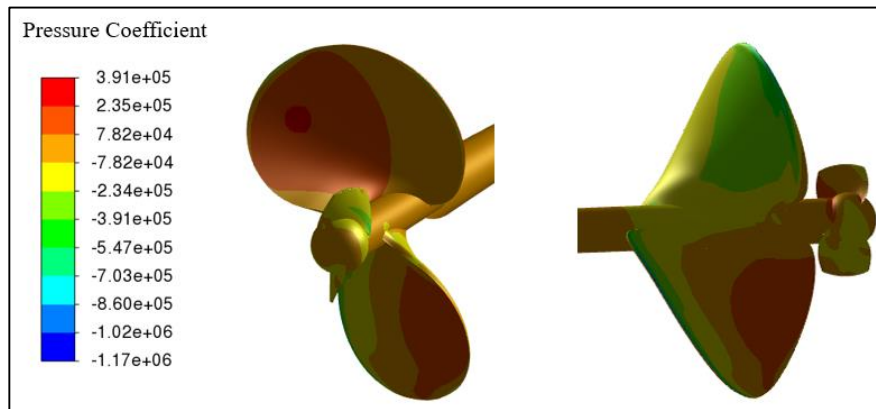

Fig. 18 Pressure distributions on pressure side (left) and suction side (right) at the blades, fins, and boss cap of TLTBP with PBCF-B operating inclined shaft condition at design advance coefficient, J=1.1

the propeller performance with PBCF-B is better than PBCF-A at each range of advance coefficients including at the design advance coefficient, J=1.1. The thrust, torque coefficients, and propeller efficiency without and with PBCF are presented in Fig. 16, where that results have corresponded in Fig. 15. At the design point, the efficiency can be increased by about 2.4% and 3.7% with PBCF-A and PBCF-B respectively.

Fig. 17 presents the component effects of the PBCF-A and PBCF-B for the TLTBP. It found the ΔK_T(Propeller Blades) for both PBCF are always positive but the values of PBCF-B are higher than PBCF-A equal to 1% - 2% of K_T(Total). ΔK_T(Boss) and ΔK_T(Long Shaft) for both PBCF are the same tendencies, and the values are minimal. The ΔK_T(Boss Cap) for both PBCF is similar, the magnitudes are positive at low speed (lower advance coefficient) and the magnitudes are negative
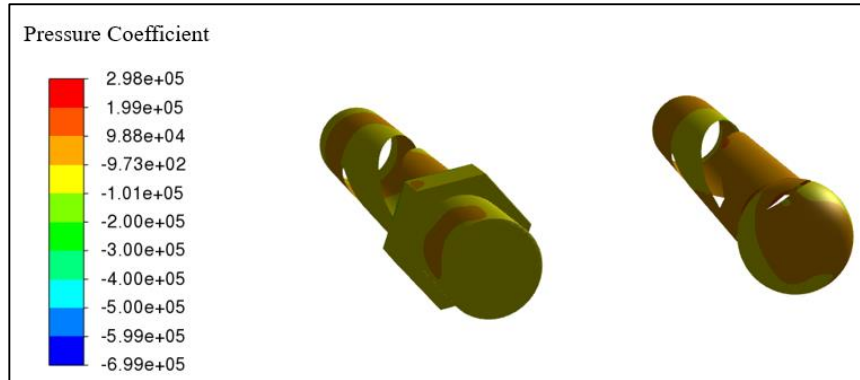
Fig. 19 Pressure distributions on the boss and boss cap of TLTBP without PBCF (left) and with PBCF-B (right) operating inclined shaft condition at design advance coefficient, J=1.1

at high speed (higher advanced coefficient). However, it seemed the ΔK_T(Boss Cap) for PBCF-A is better than PBCF-B. The ΔK_T(Fins) for both PBCF are always negative but the magnitudes of PCBF-B are slightly higher than PBCF-A by approximately 1.3% - 4.7% and 1% - 3.8% of K_T(Total) respectively.

Meanwhile, ΔK_Q(Propeller Blades) are continuously negative at each range of advance coefficients for both PBCF which, the magnitudes of PBCF-A and PBCF-B are about 0.5% - 1.5% and 0.6% - 2.3% of ΔK_q(Total) respectively, therefore, PBCF-B can be reduced the influent of propeller torque more than PBCF-A. The values of ΔK_Q(Boss), ΔK_Q(Boss Cap), and ΔK_Q(Long Shaft) with both PBCF are very small comparing to K_Q(Total). ΔK_Q(Fins) for the PBCF-A and PBCF-B are negative and the magnitudes showed by approximately 0.6% - 1.5% and 1.2% -2.4% of K_Q(Total) respectively. These results found ΔK_T(Propeller Blades) is increased, ΔK_Q(Propeller Blades) is decreased, the magnitudes of ΔK_Q(Fins) can be subsided the propeller torque while the values of others are very low therefore increasing propeller efficiency.
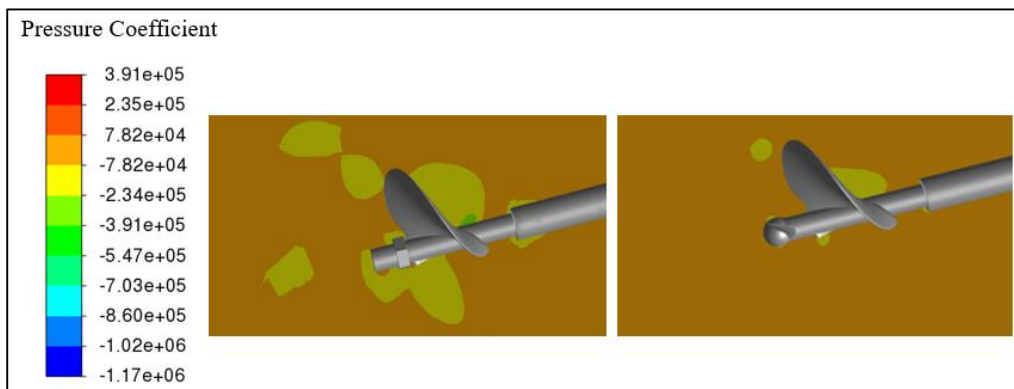

Fig. 20 Pressure distributions behind the TLTBP without PBCF (upper) and with PBCF-B (lower) operating the inclined shaft condition at design advance coefficient, J=1.1
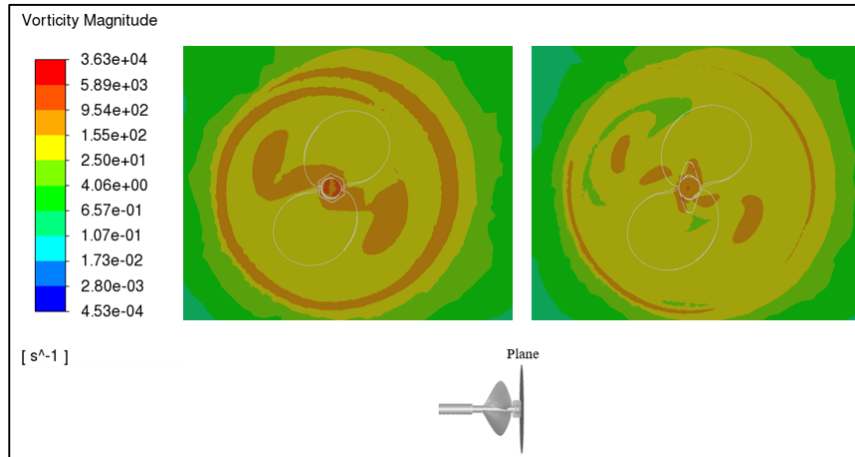
Fig. 21 Comparison of vorticity magnitude distributions between without PBCF (left) and with PBCF-B (right) on the disc area at the end of boss cap operating inclined shaft condition at design advance coefficient, J=1.1
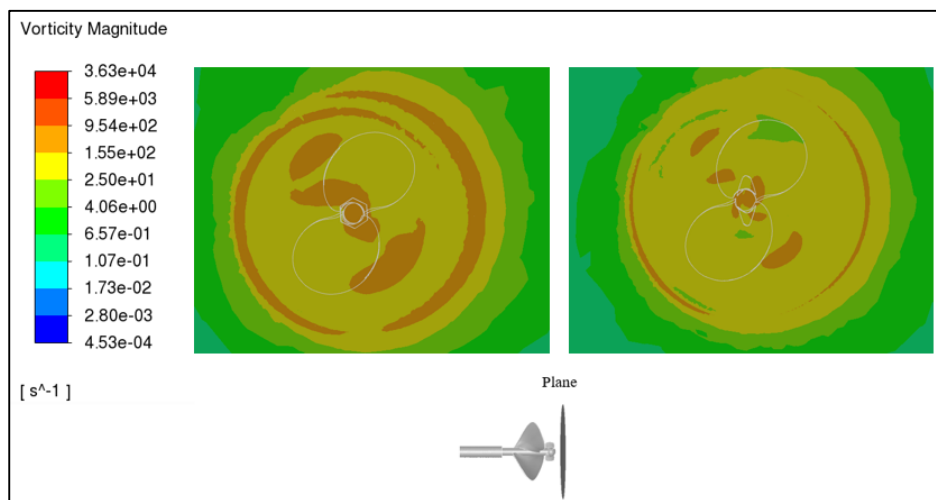

Fig. 22 Comparison of vorticity magnitude distributions between without PBCF (left) and with PBCF-B (right) on the disc area about 0.11D from the end of boss cap operating inclined shaft condition at design advance coefficient, J=1.1

The above results can found that the performance of PBCF-B has satisfied more than PBCF-A then it is suitable for matching with the TLTBP. The pressure distributions on the surface for pressure and suction sides of the TLTBP with PBCF-B operating inclined shaft condition at the design advance coefficient is shown in Fig. 18. It seemed the pressure forces of the propeller blades and fins are generated in the opposite direction, so fins generated the thrust and torque to opposite the propeller blades. These characteristics of flow fields are to break down the vortex behind fins. Fig. 19 shows the comparisons of pressure distribution on the boss and boss cap between without
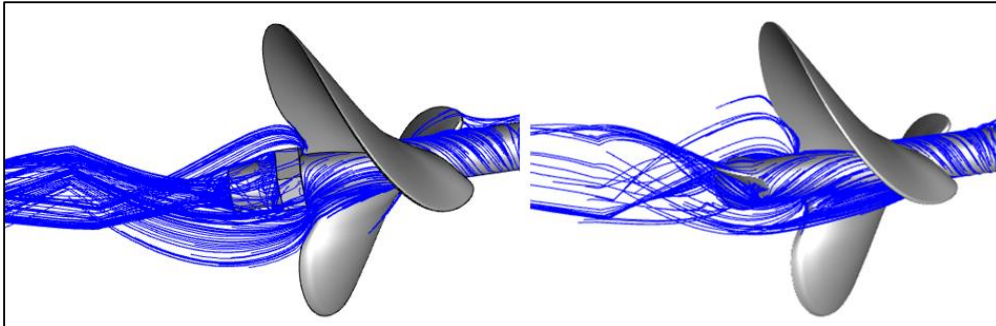
Fig. 23 Streamlines behind the boss cap of TLTBP without PBCF (left) and with PBCF-B (right) operating inclined shaft condition at design advance coefficient, J=1.1

PBCF and with PBCF-B operating inclined shaft condition. It found the average values of negative pressures for without PBCF are more than to with PBCF-B, so the fins reduced the negative pressures. The high rotation of TLTBP and boss cap will generate the negative pressure around the end of the propeller center axial which causes the hub vortex. The pressure distributions of flows behind the boss cap between without PBCF and with PBCF-B is presented in Fig.20. It is observed that the negative pressures of flows at the end of the boss cap are appeared for without PBCF but it disappears for PBCF-B, the hub vortex has been diminished.

The effects of PBCF on wake-field are analyzed through vorticity magnitude contours of fluid flows at two different plane areas between without PBCF and with PBCF-B. Fig. 21 shows the vorticity of flows on the plane area at the end of the boss cap. It is seen that the average vorticity for PBCF-B significantly reduced at the plane center but it is cannot found this phenomenal flows for without PBCF. Fig. 22 presents the vorticity of theirs on the plane area at the down steam where is located by about 0.11D from the end of the boss cap. It found the average vorticity without PBCF is higher than with PBCF-B at the plane center. Meanwhile, it is disappeared for PBCF-B which corresponded in Fig. 21. The reason, fins have broken down the vortex from the propeller boss and boss cap, therefore one solution for the reduction of the vortex is to apply the PBCF.

Fig. 23 demonstrates the streamline behind the boss cap, the shape of flows is analogous to the straight shaft condition in Fig.13. This observation in the case of without PBCF, vortex flows have appeared with hard swirling and strong in downstream. But, in the case of PBCF-B, the vortex shows to soften the aggressive of hub vortex which it is diminished vorticity by fins.

6. Conclusions

The CFD results of propeller performance for full-scale TLTBP in straight shaft condition were compared to the model-scale and experiment at each range of advance coefficients. It found the numerical results of the full-scale are a good agreement to model-scale including measured data.

The numerical analysis of the TLTBP performance between without PBCF and with two different models of PBCF in full-scale of Reynolds number in operating straight shaft condition, it is found the effects of PBCF-B are satisfied to TLTBP more than PBCF-A. The integrative for TLTBP and PBCF-B can be able to decrease propeller torque coefficients and it slightly increased propeller thrust coefficients wherefore propeller efficiency is grown by about 2.1% - 3.8%. Besides, at the

design point, the propeller efficiency is increased by approximately 2.5%. Each component analysis of PBCF-B for TLTBP found ΔK_T(Fins) is always negative, and the magnitudes are about 1% - 5% of K_T(Total), ΔK_T(Propeller Blades) are mostly positive, but the values are small with comparing K_T(Total), ΔK_T(Boss) and ΔK_T(Long Shaft) are very low. The ΔK_T(Boss Cap) showed positive at lower advance coefficients but it showed negative at higher advance coefficients. ΔK_Q(Fins) showed negative and magnitudes are about 1.0% - 2.1% of K_Q(Total), ΔK_Q(Propeller Blades) are always negative and its value by about 0.2% - 0.8% of ΔK_Q(Total). The magnitudes of ΔK_Q(Boss), ΔK_Q(Boss Cap), and ΔK_Q(Long Shaft) are very small. Consequently, their results can be described ΔK_T(Propeller Blades) are grown up but ΔK_Q(Propeller Blades) are down, while the others are small therefore, it is increasing propulsive efficiency.

The computational studies of TLTBP performance between without PBCF and with the two different models of PBCF operating inclined shaft condition, it is found that the effect of each component for PBCF-B is most suitable to TLTBP. The integrative for TLTBP and PBCF-B decreased propeller torque coefficients by about 0.6% - 2.2% and it increased propeller thrust coefficients by about 1.0% - 2.5% so propeller efficiency can be grown up by about 1.6% - 4.4%. Furthermore, the efficiency is increased by approximately 3.7% at the design point. The component effects of PBCF for TLTBP-B are evaluated that, ΔK_T(Boss Cap) is positive at lower advance coefficients and negative at higher advanced coefficients, ΔK_T(Propeller Blades) is always positive, and the values are about 1.0% - 2.6% of K_T(Total), ΔK_T(Boss) and ΔK_T(Long Shaft) are low. ΔK_Q(Fins) is negative at all, and its value by approximately 1.2% - 2.4% of K_Q(Total), ΔK_Q(Propeller Blades) are continuously negative at each range of advance coefficients, and the magnitudes are about 0.6% -2.3% of K_Q(Total) while ΔK_Q(Boss), ΔK_Q(Boss Cap), and ΔK_Q(Long Shaft) are very small. This phenomenal of flows are influent into the positive of ΔK_T(Propeller Blades), but ΔK_Q(Propeller Blades) is always negative, and the others are small. Furthermore, ΔK_Q(Fins) diminished the total torque thus it can be summarized that the vortex from the propeller boss and boss cap have subsided by application of fins wherefore increased propulsive efficiency.

Acknowledgments

References

Abar, I. and Utama, I.K. (2019), "Effect of the incline angle of propeller boss cap fins (PBCF)", *Int. J. Technol.,* **10**(5), 1056-1064. https://doi.org/10.14716/ijtech.v10i5.2256.

Alder, R.S. and Moore, D.H. (1977), "Performance of An Inclined Shaft Partially-Submerged Propeller Operating Over A Range of Shaft Yaw Angle"*s*, David W. Taylor Naval Ship Research and Development Center, Bethesda, Maryland, USA.

Bal, S. (2020), "Inclination angle influence on noise of cavitating marine propeller", *Ocean Syst. Eng.*, **10**(1), 49-65. https://doi.org/10.12989/ose.2020.10.1.049.

Dubbioso, G., Muscari1, R. and Di Mascio, A. (2013), "CFD Analysis of propeller performance in oblique flow", *Proceedings of the 3rd International Symposium on Marine Propulsors (smp'13)*, Launceston,

Tasmania, Australia.

Gaggero, S. and Villa, D. (2018), "Cavitating propeller performance in inclined shaft conditions with OpenFOAM: PPTC2015 test case", *J. Mar. Sci. Appl.*, **17**, 1-20. https://doi.org/10.1007/s11804-018-0008-6.

Ghassemi, H., Mardan, A. and Ardeshir, A. (2012), "Numerical analysis of hub effect on hydrodynamic performance of propellers with inclusion of PBCF to equalize the induced velocity", *Pol. Marit. Res.,* **19**(2), 17-24. https://doi.org/10.2478/v10012-012-0010-x.

Kaewkhiaw, P., Yoshitake, A., Kanemaru, T. and Ando, J (2015), "Experimental and numerical study of propeller performance for Long-Tail Boat in Thailand", *Japan Soc. Naval Archit. Ocean Engineers*, **20**, 407-410.

Kaewkhiaw, P., Yoshitake, A., Kanemaru, T. and Ando, J. (2016), "Evaluation of Thai Long-Tail Boat propeller performance and its improvement", *Proceedings of the 12th International Conference on Hydrodynamics (ICHD)*, Netherlands.

Kaewkhiaw, P. (2020), "CFD analysis of unsteady propeller performance operating at different inclined shaft angles for LONG-TAIL boat in Thailand", *J. Nav. Archit. Mar. Eng.*, **17**(2), 115-127. http://doi.org/10.3329/jname.v17i2.42622.

Katayama, Toru., Nishihara, Yoshitaka. and Sato, Takuya. (2013), "Study On The Characteristics of Self-Propulsion Factors of Planing Craft With Outboard Engine", Article in Transactions of SNAME.

Kawamura, T., Ouchi, K. and Nojiri, T. (2012), "Model and full scale CFD analysis of propeller boss cap fins (PBCF)", *J Mar Sci Technol.*, **17**, 469-480. https://doi.org/10.1007/s00773-012-0181-2.

Krasilnikov, V., Zhang, Z. and Hong, F. (2009), "Analysis of unsteady propeller blade forces by RANS", *First International Symposium on Marine Propulsors (smp'09)*, Trondheim, Norway.

Lim, S.S., Kim, T.W., Lee, D.M., Kang, C.G. and Kim, S.U. (2014), "Parametric study of propeller boss cap fins for container ships", *Int. J. Nav. Archit. Ocean Eng.*, **6**, 187-205. http://dx.doi.org/10.2478/IJNAOE-2013-0172.

Nojiri, T., Ishii, N. and Kai, H. (2011), "Energy saving technology of PBCF and its evolution", *Japan Inst. Mar. Eng.*, **46**(3), 350-358. https://doi.org/10.5988/jime.46.350.

Peng, C.H., Cheng, M., Ke, C., Fang1, Q.Z. and Jun, Y.C. (2013), "An integrative design method of propeller and PBCF", *Proceedings of the 3rd International Symposium on Marine Propulsors (smp'13)*, Launceston, Tasmania, Australia.

Peck, J.G. and Moore, D.H. (1973), "Inclined-Shaft Propeller Performance Characteristics", Report of SNAME, New York, USA.

Ryu, T., Kanemaru, T., Kataoka, S., Arihama, K., Yoshitake, A., Arakawa, D. and Ando, J. (2014), "Optimization of energy saving device combined with a propeller using real-coded genetic algorithm", *Int. J. Nav. Archit. Ocean Eng.*, **6**, 406-417. http://doi.org/10.2478/IJNAOE-2013-0188.

Schroeder, S. and Dai, C. (2010), "Numerical Simulation of Propeller Performance With An Inclined Shaft Arrangement", Report of Naval Surface Warfare Center Carderock Division, West Bethesda, USA.

Seo, J., Lee, S.J., Han, B. and Rhee, S.H. (2016), "Influence of design parameter variations for propeller-boss-cap-fins on hub vortex reduction", *J. Ship Res.*, **60**(4). http://doi.org/10.5957/JOSR.60.4.160003.

Shields, Curtis E. (1965), "Open-Water Propeller Performance in Inclined Flow", David W. Taylor Naval Ship Research and Development Center, Bethesda, Maryland, USA.

Sun, Y., Su, Y., Wang, X. and Hu, H. (2016), "Experimental and numerical analyses of the hydrodynamic performance of propeller boss cap fins in a propeller rudder system", *Eng. Appl. Comput. Fluid Mech.*, **10**, 145-159. https://doi.org/10.1080/19942060.2015.1121838.

Taniguchi, K., Tanibayashi, H. and Chiba, N. (1969), *Investigation Into The Propeller Cavitation In Oblique Flow*, Mitsubishi Technical Bulletin.

MK

Nomenclature

TLTBP	:	Thai Long-Tail Boat propeller
PBCF	:	Propeller boss cap fin
CFD	:	Computational fluid dynamics
RANS	:	The Reynolds-averaged Navier-Stokes equations
k-ω SST	:	Shear Stress Transport k-ω
$K_T = \dfrac{\text{Thrust}}{\rho n^2 D^4}$	:	Thrust coefficient
$K_q = \dfrac{\text{Torque}}{\rho n^2 D^5}$	:	Torque coefficient
$J = \dfrac{V_a}{nD}$	:	Advance coefficient
$C_p = \dfrac{P - P_o}{\frac{1}{2}\rho n^2 D^2}$	:	Pressure coefficient
P	:	Pressure on the blade
P_o	:	Pressure at infinity
n	:	Propeller rotational speed
V_a	:	Inflow velocity
η_o	:	Propeller efficiency
ρ	:	Density of fluid
r	:	Thai Long-Tail Boat propeller radius
D	:	Thai Long-Tail Boat propeller diameter
φ	:	Inclined shaft angle